Geothermal Setting and Simple Heat Conduction Models for the Long Valley Caldera

ARTHUR H. LACHENBRUCH, J. H. SASS, ROBERT J. MUNROE, AND T. H. MOSES, JR.

U.S. Geological Survey, Menlo Park, California 94025

Heat flow and heat production measurements have been made in the vicinity of Long Valley from 0–30 km from the rim of the caldera and up to 30 km on either side of the boundary of the Basin and Range province at the eastern scarp of the Sierra Nevada. The search for a thermal anomaly associated with magma is complicated by the location of the caldera at the boundary between these two provinces with strongly contrasting regional heat flows and by unknown effects of hydrothermal circulation. The data show no conspicuous effect of the province transition, possibly a small local heat flow anomaly near the east rim of the caldera, and a very substantial anomaly near the west rim. Simple heat conduction models suggest that Long Valley caldera is the surface expression of a deep magmatic system; an upper crustal magma chamber could not have sustained molten material throughout the 2-m.y. eruptive history unless it were resupplied with heat from deep crustal or subcrustal magmatic sources. If the heat were supplied by crustal intrusion of mantle basalt, the crust would thicken rapidly unless magmatic activity were accompanied by accelerated local crustal spreading. To generate a viable silicic magma chamber by sill injection in the upper 5–8 km of crust, minimum intrusion rates of the order of 1 m per century are probably required. Thermal models for the near-normal heat flow at the east rim suggest that magma beneath the eastern part of Long Valley caldera might have been exhausted during eruption of the Bishop Tuff 0.7 m.y. ago and that the resurgent dome, which subsequently formed in the west central caldera, marks the location of a residual chamber more circular in plan. High heat flow indicated by the single measurement near the west rim can be attributed to a simple shallow magma chamber beneath the western caldera or to recent local magmatism along the Sierra frontal fault system. Additional heat flow and hydrologic measurements are necessary for a confident interpretation of the thermal history and the present state of the caldera region.

INTRODUCTION

As part of an investigation of the Long Valley region we have measured heat flow in 11 holes drilled to depths of 150–300 m in terrain surrounding the caldera (Figures 1 and 2). Our aim was to investigate any detectable effects that magmatic events associated with the caldera might have had on the conductive thermal regime of the surroundings. Because of the long time required for a thermal disturbance to equilibrate by conduction in earth materials, measurements of heat flow, unlike other geophysical measurements, can contain direct information on past geologic events. However, with the introduction of the time variable, the inverse problem of reconstructing the cause from an observation of its effects takes on an added dimension of ambiguity. Near hot spring areas a further complication in the interpretation of heat flow measurements is the uncertainty of the role played by hydrothermal convection. Indeed, the large estimates of sustained heat discharge from hot springs in Long Valley caldera and similar volcanic regions [*White*, 1965; *Sorey and Lewis*, 1976] indicate either that the magmatic source must be very close to the surface or, more reasonably, that convective transport must dominate conduction to considerable depth beneath these regions [*Lachenbruch et al.*, 1976]. Nevertheless, if heat is transferred primarily by conduction in the crystalline rocks surrounding Long Valley caldera, it should be possible to confirm this with internally consistent heat flow measurements beyond the caldera rim. Analysis of these measurements could, in principle, provide limiting information on the distribution, history, and present state of magmatic sources that might extend to the edge of the caldera or beyond. In any case, if we neglect heat transfer by hydrothermal convection, useful limits can be calculated for the time required for any hypothetical magma source to cool. Simple conduction models are used in this paper to make approximate calculations of these kinds (i.e., of present state and maximum cooling time). Analytical results are presented in a general graphical form somewhat more complete than is warranted for interpretation of our preliminary measurements near Long Valley; the problems are general, and it is expected that the results might be useful for similar calculations applicable elsewhere.

The new thermal data are summarized in Table 1; they were obtained by procedures described by *Sass et al.* [1971*a*, *b*]. The heat production (A_0) was measured by our colleague Carl Bunker, using the methods of *Bunker and Bush* [1966, 1967]. The heat flows (q) are based on linear least squares temperature gradients (Γ) over the specified depth intervals, corrected (to Γ_c) where appropriate for the effects of topography, uplift, erosion, and glaciation, and multiplied by harmonic mean thermal conductivities ($\langle K \rangle$). Inasmuch as a significant fraction of the data is based on temperature profiles acquired shortly after the access pipe was grouted in, we have omitted the customary formal statistical estimates of scatter from the least squares mean gradients and consequently from estimates of mean thermal conductivity, heat flow, and radiogenic heat production (A_0). Adjustments to these preliminary values based on equilibrium temperature gradients and an increased number of conductivity and heat production measurements are anticipated. The units of heat flow (HFU), units of heat production (HGU), and units of thermal conductivity (CU) are defined in Table 1.

The latest temperature measurements from each of the new holes is shown in Figure 3*a*. In Figure 3*b*, profiles from the 10 holes in granitic rock are plotted in such a way that the portions used to determine heat flow extrapolate to a common origin at the surface.

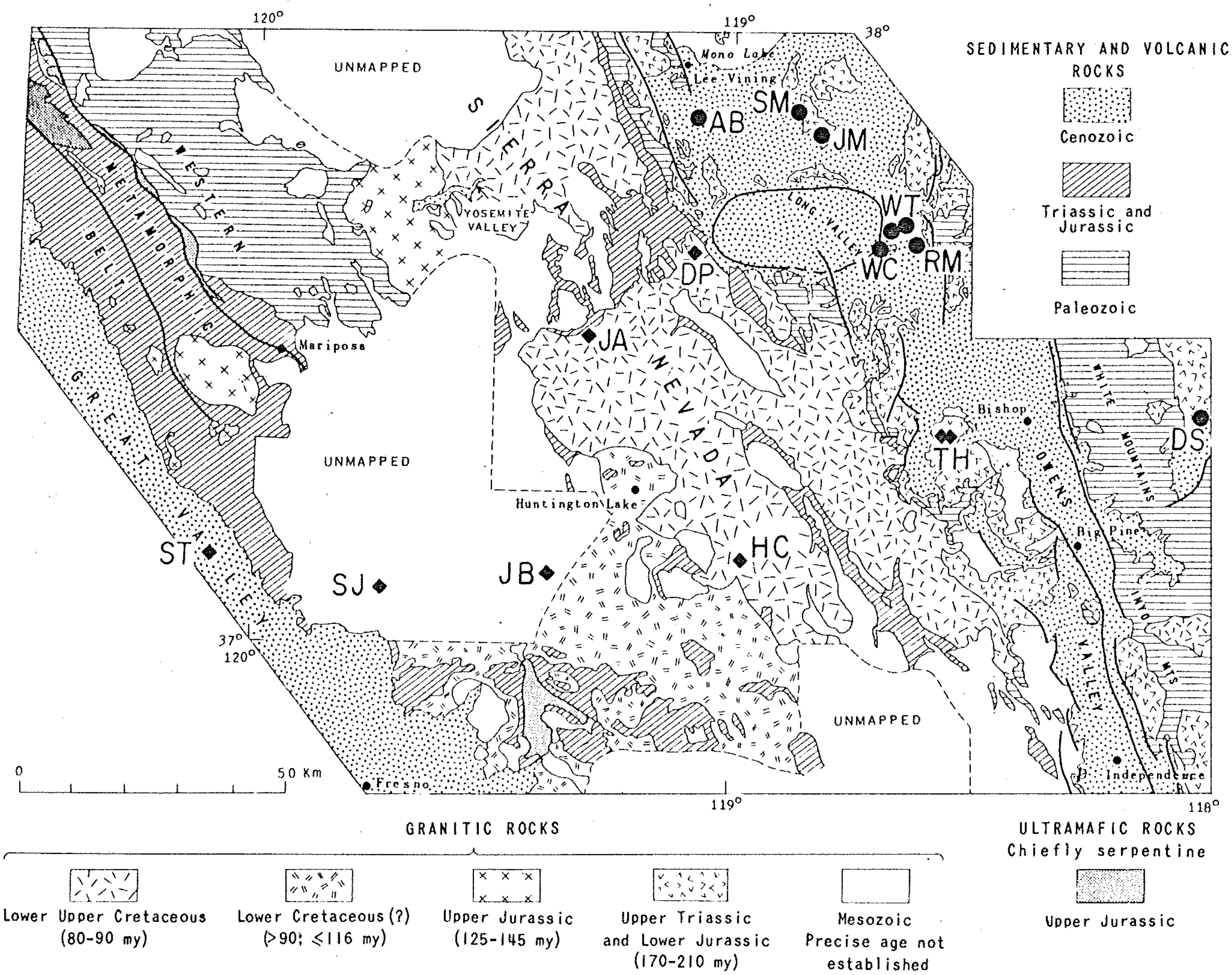

Fig. 1. Geologic sketch map [after *Bateman and Eaton*, 1967] showing outline of the Long Valley caldera and locations of heat flow stations. Square symbols are identified with the Sierra Nevada physiographic province; circles, with the Basin and Range province. (Results from ST, SJ, JB, HC, and DS have been published previously.)

THERMAL SETTING OF LONG VALLEY

As explained by *Bailey et al.* [1976], the Long Valley caldera lies nearly astride a major fault system that separates the tectonically active Basin and Range province to the east from the relatively stable Sierra Nevada tectonic province to the west. The Basin and Range province is characterized by extensive Cenozoic normal faulting and volcanism, high seismicity, a thin crust, and a low upper mantle seismic velocity; none of these characteristics obtain in the Sierra Nevada [*Thompson and Burke*, 1974; *Bateman and Eaton*, 1967; *Pakiser and Robinson*, 1966]. Consistent with these tectonic indicators, the contrast in regional heat flow across this boundary is one of the most abrupt known on the North American continent [*Roy et al.*, 1968, 1972; *Sass et al.*, 1971*a*]. While this location makes Long Valley an interesting subject for study, the transition zone compounds the problem of establishing the regional heat flow upon which any local anomaly might be superimposed.

The problem of establishing the background heat flow is simplified somewhat by the observation that heat flow q from granitic rocks in each province generally depends to a first approximation on the radiogenic heat production A_0 of the rock locally exposed at the surface according to the following relation [*Birch et al.*, 1968; see also *Roy et al.*, 1968; *Lachenbruch*, 1968*c*].

$$q = q^* + DA_0 \qquad (1)$$

The parameters (q^*, D) have the respective dimensions of heat flow and depth, and they may be viewed as uniform throughout each province (although the relation is much less certain for the Basin and Range [*Roy et al.*, 1968, 1972; *Blackwell*, 1971]). For the Sierra Nevada the values are 0.4 HFU and 10 km, and for the Basin and Range they are 1.4 HFU, 10 km. The second term in (1) is equivalent to the steady heat flux that would be produced by a uniform 10-km slab of the rock currently exposed locally at the surface [*Roy et al.*, 1968]. It is determined by multiplying by 10 km the heat production (per cubic kilometer) determined by a laboratory measurement on core or surface samples. The expected heat flow is then determined by adding 0.4 HFU (q^*, equation (1)) if the station is in the Sierra Nevada or 1.4 HFU if it is in the Basin and Range province. Hence this unexpected relation implies that the rock exposed locally at the surface contains information on the heat flow and thermal regime of the entire crust.

It seems unlikely that granites of greatly varying age in a given province would all have the same thickness D (in these cases, 10 km). It has been shown, however, that (1) will not be affected by differential erosion in any province if (and only if) the heat production, instead of being uniform to depth D, varies with depth z according to $A_0e^{-z/D}$ [*Lachenbruch*, 1968*a*,

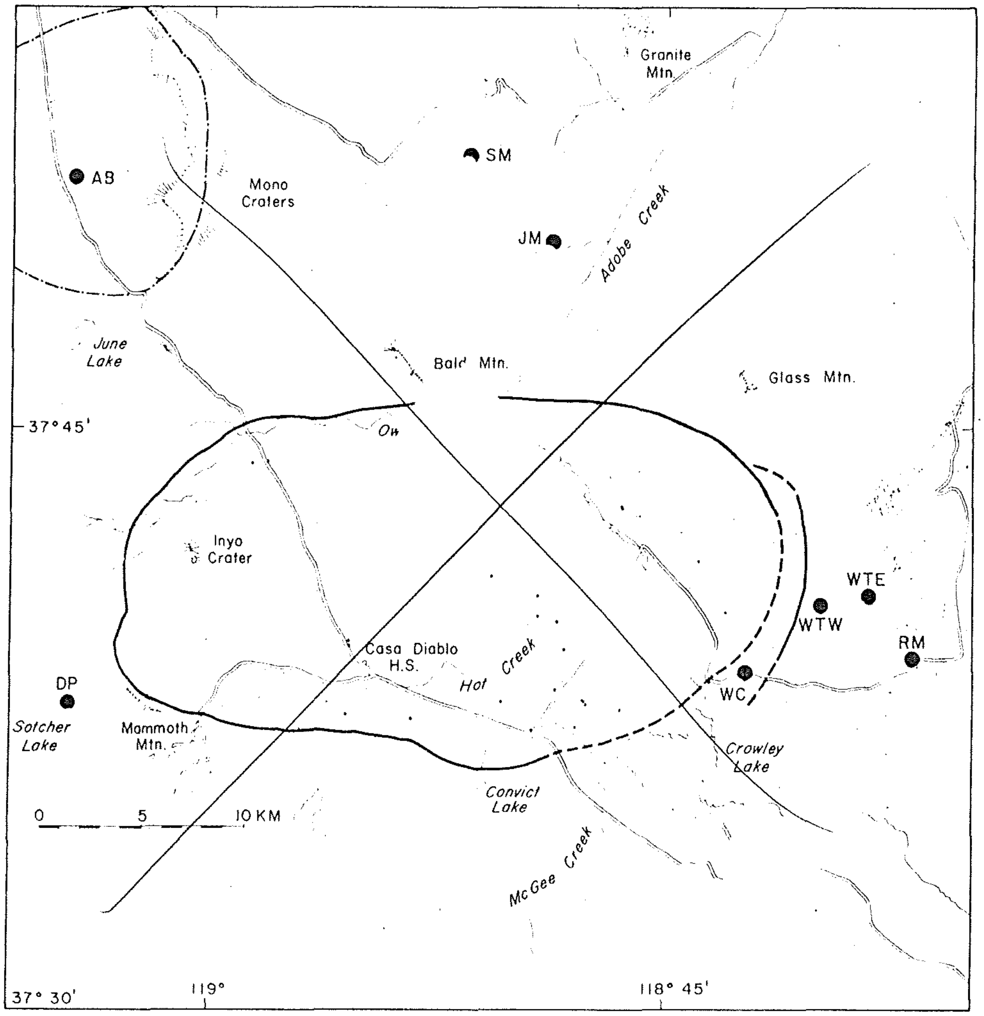

Fig. 2. Sketch showing the location of close-in heat flow stations relative to the caldera rim and other major physiographic features. Chain-dotted line at upper left outlines the ring fracture zone of *Kistler* [1966]. The small dots inside the caldera show the locations of heat flow and hydrological data discussed by *Lachenbruch et al.* [1976].

1970]. With this interpretation, q^* is most naturally identified as the contribution from the mantle. A knowledge of the province parameters (q^*, D) and an assumption of conductivity then lead to a complete crustal temperature profile from a knowledge of surface heat flow or heat production. Such profiles are shown in Figure 4 for the Sierra Nevada and the Basin and Range for the extremes of heat production normally found in plutonic rocks (0–10 HGU) and for

TABLE 1. Summary of Preliminary Geothermal Data Near Long Valley, California

Site	Elevation, m	Depth Range, m	Γ, °C/km	Γ_c, °C/km	$\langle K \rangle$, CU	q, HFU	A_0, HGU	Q_S,* HFU	Q_{BR},† HFU	Distance Beyond Rim, km
Jackass Creek (JA)	2100	60–190	17.7	18.7	7.26	1.36	9.6	0	(−1.0)	28 (SW)
Devils Postpile (DP)	2316	150–250	56.8	51.4	7.30	3.75	6.0	2.75	(1.75)	3 (WSW)
Tungsten Hills (THE)	1737	160–189	15.1	14.7	6.35	0.93	3.1	0.2	(−0.8)	30 (S)
Tungsten Hills (THW)	1760	100–138	15.1	14.4	8.8	1.27	6.8	0.2	(−0.8)	30 (S)
Aeolian Buttes (AB)	2240	25–124	31.2	31.2	6.98	2.18	8.7	(0.9)	−0.1	13 (NNW)
Watterson Canyon (WC)	2133	110–140	30.0	30	7.44	2.23	4.2	(1.4)	0.4	0 (SE rim)
Watterson Trough (WTW)‡	2316	50–113	78.1	78.1	2.7	2.1				1 (E)
Watterson Trough (WTE)	2393	90–128	23.0	25.0	6.70	1.68	4.4	(0.8)	−0.2	3 (E)
Round Mountain (RM)	2225	125–209	24.3	24.0	7.91	1.90	7.7	(0.7)	−0.3	6 (E)
Johnny Meadow (JM)	2637	100–168	6.08	6.1	6.75	0.41	6.4	(−0.6)	−1.6	6 (N)
Sagehen Meadow (SM)	2560	150–271	9.20	9.3	7.79	0.72	9.3	(−0.6)	−1.6	11 (N)

1 conductivity unit (CU) = 1 mcal cm^{-1} s^{-1} °C^{-1} = 0.418 W m^{-1} °K^{-1}; 1 heat flow unit (HFU) = 1 μcal cm^{-2} s^{-1} = 41.8 mW m^{-2}; 1 heat generation unit (HGU) = 10^{-13} cal cm^{-3} s^{-1} = 0.418 μW m^{-3}.

* Q_S is heat flow anomaly relative to the Sierra Nevada norm. Values in parentheses are for sites in the Basin and Range physiographic province.

† Q_{BR} is heat flow anomaly relative to the Basin and Range norm. Values in parentheses are for sites in the Sierra Nevada physiographic province.

‡ Drilled in rhyolitic tuff; all other holes were drilled in granitic rocks.

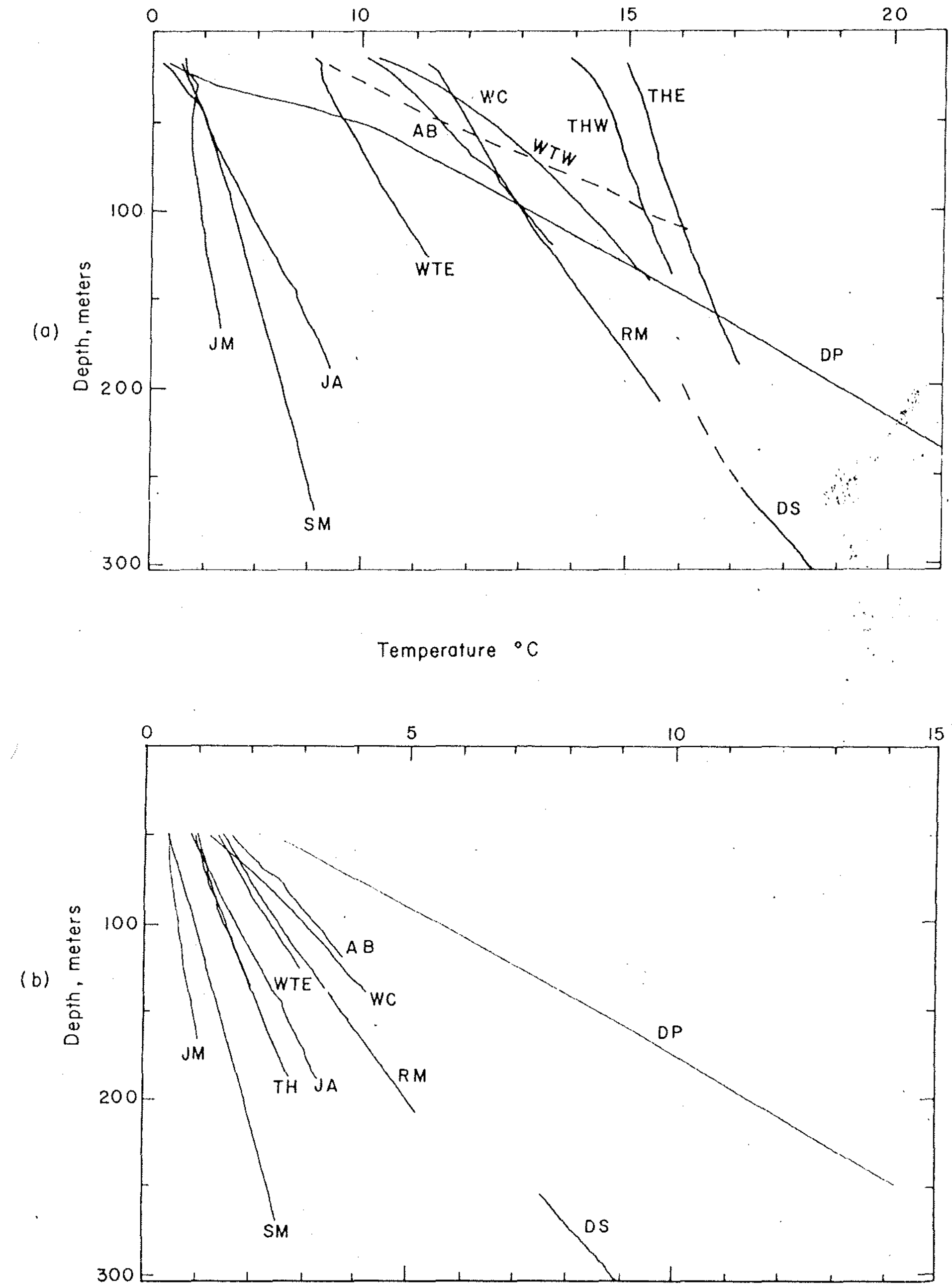

Fig. 3. Temperature profiles from holes near Long Valley: (*a*) all profiles and (*b*) profiles from holes in granite with their extrapolated surface temperatures adjusted to a common origin.

assumed conductivities believed reasonable for each province. For the same surface heat production, heat flow will generally be greater by 1 HFU at sites in the Basin and Range. For the same surface heat flow (e.g., 1.4 HFU, Figure 4) crustal temperatures are much higher in the Basin and Range because a larger proportion of the heat originates at great depth there.

In Figure 5, measured values of (q, A[illegible]) are plotted for each of the stations in granitic rock shown in Figure 1. The straight lines represent relation [illegible] with the appropriate slope and intercept parameters D and q* for each province. These parameters were determined previously from published investigations [illegible] [illegible] *Lachenbruch*, [illegible] [illegible] [illegible] Tungsten Hills (TH), San Joaquin (SJ), [illegible] (RC), and Deep Springs (DS) occur in the map area of Figure 1. The stations represented by squares in Figures 1 and 5 lie southwest of the physiographic boundary between the Sierra Nevada and the Basin and Range; those represented by circles lie northeast of it. This assignment to province is unambiguous at all stations except perhaps at the two sites at Tungsten Hills (THE and THW). Table 1 lists the 11 new sites, roughly in order of increasing distance from the physiographic boundary, distance within the Sierra Nevada province being considered negative.

The departure of the circles and squares in Figure 5 from their respective province norms (the straight lines) can be viewed as the measure of a local heat flow anomaly. The anomaly may reflect several contributing causes, and perhaps [illegible]. First, the data from the Basin and Range generally show considerable local scatter about their curve; the five upper circles in Figure 5 are not atypical. Second, many of the points lie close to the boundary of the two provinces.

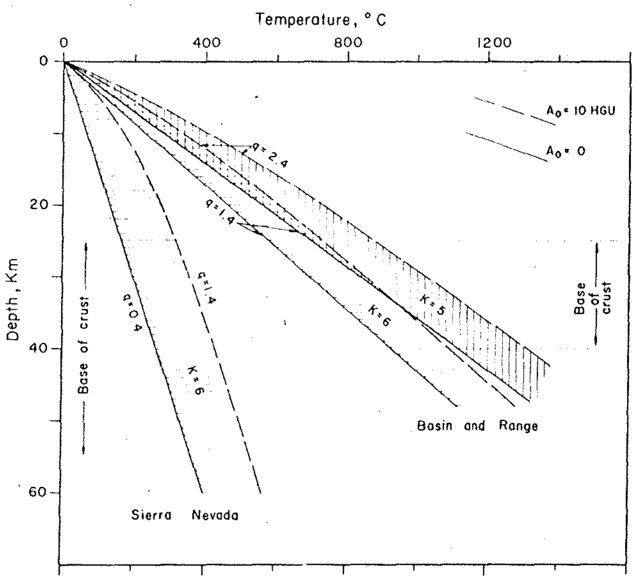

Fig. 4. Theoretical steady state crustal temperature profiles based on the exponential source model and the heat flow–heat production relationship inferred for the Sierra Nevada and Basin and Range heat flow provinces [*Lachenbruch*, 1970]. Horizontal screen represents an assumed thermal conductivity of 6 CU, vertical screen represents 5 CU. A_0 and q represent surface heat production in heat generation units and surface heat flow in heat flow units, respectively. (For definitions of units, see Table 1.)

where the deep crustal heat flow (q^*) must change by a factor of 3 or more. As this change must be transitional in some degree, we should expect such points normally to lie between the two province curves. Third, very slight systematic movements of groundwater can cause substantial anomalies (positive or negative) in the conductive heat flow. Where the upper crust contains local anomalous sources of heat, such circulation is more likely to be important. Finally, most of the points in Figure 5 are based on preliminary data, and their plotted positions may be revised when additional measurements are made. With these qualifications it is still rather surprising that with the exception of Johnny Meadow (JM), Sagehen Meadow (SM), and Devils Postpile (DP), Figure 5 does not show conspicuous anomalies. In Table 1 the anomalies relative to the Sierra and Basin and Range norms are tabulated, respectively, under Q_S and Q_{BR}.

It is not surprising that ST, SJ, JB, and HC lie on the Sierra curve because they were among the previously published points used to define it [*Roy et al.*, 1968; *Lachenbruch*, 1968*a*]. It is surprising that THE and THW, which lie almost on the physiographic boundary, do not show a stronger effect of the transition. However, they are based upon incomplete conductivity and heat production data. The new site at Jackass Creek (JA) in the central Sierra Nevada lies precisely on the previously established Sierra curve. This observation not only provides important confirmation for (1), but it also establishes that at this site, 28 km southwest of Long Valley caldera, there are no detectable thermal effects of the Long Valley igneous activity, the basaltic volcanism that preceded it by 2 or 3 m.y., or any transition to the Basin and Range thermal regime. The Sierra point, DP, at Devils Postpile (Figures 1 and 2) 25 km northwest of JA and 3 km from the caldera rim, shows a very conspicuous anomaly, as it lies 2.75 HFU above the Sierra curve (Figures 3 and 5; Table 1). The conductive heat flow at DP is well determined in homogeneous competent rock by a smooth and uniform gradient (Figure 6). The slight curvature in the upper half of the profile in quartz monzonite at this important site can be accounted for by local topography.

We have mentioned that the departure of the five upper circles (Figure 5) from the Basin and Range line is not atypical for the province. This group includes sites whose distance from the caldera varies from ~0 at Watterson Canyon (WC) to 70 km at DS and whose distance from the physiographic boundary varies from less than 10 km at Aeolian Buttes (AB) to 35 or 40 km at DS. Thus there is no compelling evidence to suggest that the circles a bit below the Basin and Range line are transitional because of their proximity to the province boundary. The fact that the highest heat flow (2.2 HFU) in the Basin and Range group occurs at the site (WC) on the eastern caldera rim seems to suggest that a small local conductive anomaly might occur there. The value of 2.1 HFU in nearby tuff at Watterson Trough (WTW) (Table 1), though uncertain, lends a little support to that view. However, at these locations near the rim, effects of thermal refraction could easily account for local variations of a few tenths of a HFU [see, e.g., *Lachenbruch*, 1968*b*, p. 399]; corrections for them are not warranted because of the other sources of uncertainty. The two very low heat flows at SM and JM are puzzling and evidently reflect hydrologic effects. Our inability to account for them at this time serves as a reminder of the uncertainty in these results.

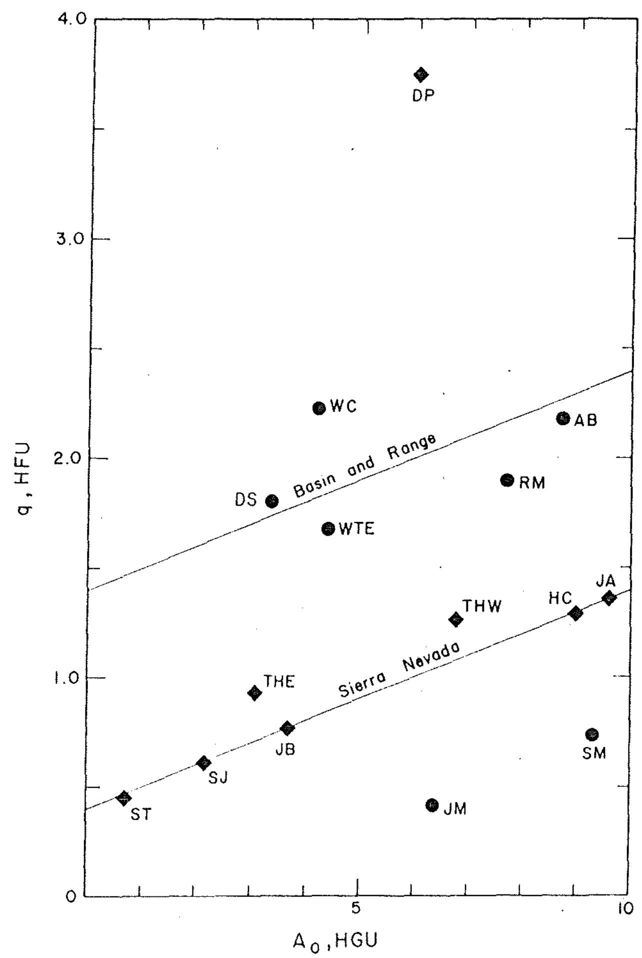

Fig. 5. Heat flow versus heat production for granitic rocks in the region surrounding Long Valley. Square symbols are identified with the Sierra Nevada physiographic province; circles, with the Basin and Range province. The straight lines represent previously determined relationships (equation (1)) for the two provinces [*Roy et al.*, 1968; *Lachenbruch*, 1968*a*].

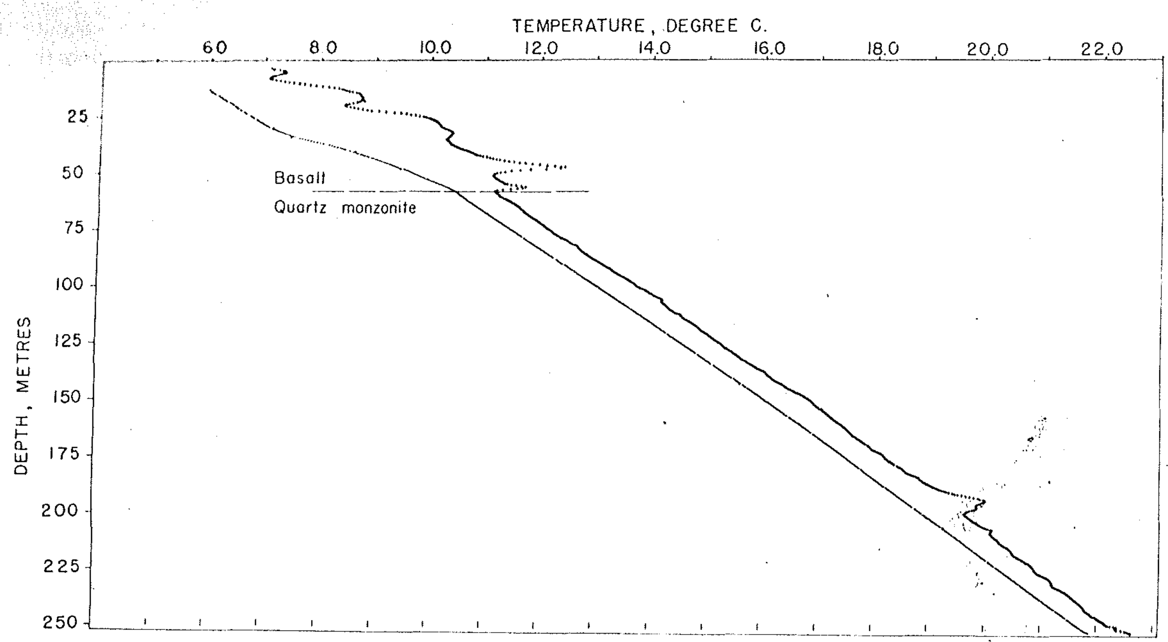

Fig. 6. Temperature profiles from DP. The upper profile (showing thermal effects of cementing) was obtained a day after completion of the hole; the lower profile, 9 months later.

In summary, the preliminary thermal data show no conspicuous effect of the province transition, possibly a very small local conductive anomaly at the east rim of Long Valley caldera, and a very substantial one a few kilometers beyond the west rim. Recognizing that these generalizations are tentative, in the next section we shall attempt to analyze some of their implications with the aid of geologic information relating to the history of the caldera.

IMPLICATIONS FOR THE MAGMATIC HISTORY OF LONG VALLEY CALDERA

Some relevant geologic information. According to *Bailey et al.* [1976], Long Valley caldera resulted from the collapse of the roof of a magma chamber during the explosive eruption of a layer of partially crystallized magma (the Bishop Tuff) perhaps 2 km thick about 0.7 m.y. ago. The Long Valley magma chamber is thought to be more or less congruent in plan with the caldera structure, an ellipse with axes of about 20 and 30 km. The oldest evidence for the existence of the Long Valley magma chamber is Glass Mountain on the northeast rim of the present caldera; silicic volcanism began there almost 2 m.y. ago and continued intermittently up to the time of collapse. Shortly after the collapse a resurgent dome formed in the west central part of the caldera, and silicic and intermediate volcanic material has been discharging in and around it virtually up to the present time. The most recent activity has been concentrated near the western rim along the Sierra Nevada frontal fault system, and little or no material has been discharged in the eastern half of the caldera during the past 0.3 m.y. Basaltic volcanism in the vicinity of Long Valley predated caldera formation by as much as 3 m.y. or so, and recent basaltic volcanism along the Sierra frontal faults is evidently almost contemporaneous with the most recent silicic extrusion from the Long Valley system. Largely on the basis of mechanical arguments relating to collapse and resurgence [*Bailey et al.*, 1976; *Smith and Bailey*, 1968], the roof above the magma chamber is estimated to have been about 5 km thick. On the basis of geochemical arguments the magmatic temperature was probably about 800°C [*Hildreth and Spera*, 1974; R. L. Christiansen, personal communication, 1974].

Given this information and the preliminary heat flow results outlined above, we should like to know whether it is possible to place any useful constraints on the history of the hypothetical chamber and its present state from theoretical considerations. The problem of thermal effects of igneous intrusion is extremely complex, involving conductive and convective transport of heat in inhomogeneous geometrically complicated systems little known in detail. It is the subject of several extensive discussions [e.g., *Lovering*, 1935; *Shaw*, 1965; *Jaeger*, 1964; *Simmons*, 1967*b*] which we make no attempt to review in this preliminary study. The related problem of hydrothermal convection beneath hot springs, largely neglected in this discussion, is also the subject of an extensive literature. We consider only some simple limiting heat conduction models, most of which are well known, in an attempt to investigate the consistency of the geologic and geothermal observations and inferences to date.

Some simple conduction models. The time progression of temperature for three simple one-dimensional models of a magmatic heat source is shown schematically in Figure 7. In these models the magma chamber is a slab extending infinitely in the horizontal directions, and a represents the depth of its roof beneath the surface. In model I the magma raises the temperature of its roof Θ_0 degrees above its surroundings at time $t = 0$, and it maintains this condition thereafter ($t > 0$), as might be expected in an idealized convecting chamber. Model II is the instantaneous source model wherein magma of thickness Δ is assumed to move instantaneously into place at time $t = 0$ at a temperature Θ_0 above its surroundings; thereafter the magma stagnates and loses its heat by conduction from its upper and lower boundaries. In model III, heat is liberated at a constant rate Q_0 cal/cm² s starting at time $t = 0$ on the plane $z = a$, which represents the chamber roof. The physical significance of model III will be discussed below.

We define Q_2 as follows:

$$Q_2 = K(\Theta_0/a) \qquad (2)$$

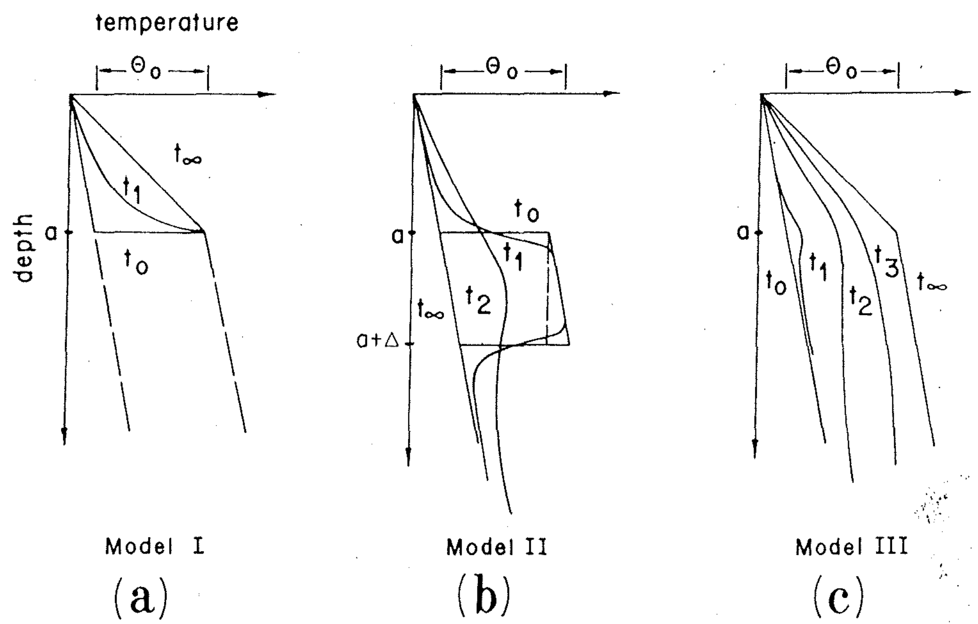

Fig. 7. Schematic representation of the time progression of temperature from the initial condition (t_0) to the steady state condition (t_∞) for three one-dimensional conduction models of a magmatic heat source (see text).

where K is thermal conductivity, assumed to be uniform. Hence after equilibrium is established, the rate of upward heat loss from models I and III will be the same.

It is convenient to discuss these heat conduction models in terms of a characteristic 'conduction length' $l(t)$ defined by

$$l(t) \equiv (4\alpha t)^{1/2} \tag{3}$$

where α, the thermal diffusivity, is the ratio of the thermal conductivity to the volume specific heat of the principal materials through which heat is being conducted. Generally, $l(t)$ represents a characteristic distance from the source of a temperature disturbance to which a perturbation is likely to be appreciable after the passage of time t. Representative values of l are presented for selected values of t and α in Table 2. The first column, denoted by l', might be appropriate for calculations principally involving conduction within the liquid magma, and possibly through the roof materials above it as well, if porous volcanic rocks and sediments predominate. The second column, l'', represents an average for conduction paths including heated and cool crystalline rocks and the more poorly conducting materials just mentioned. It may be appropriate for conduction paths related to close-in thermal edge effects around the caldera rim and also for conduction through the roof if it contains an appreciable amount of crystalline rock. The last column, l''', represents crystalline rock at average temperatures not exceeding a few hundred degrees. The fact that the thermal properties probably contrast significantly among materials in, above, and surrounding the magmatic system poses problems for simple homogeneous models. Actually, the properties of all of the materials in the system affect the temperature in any one of them, sometimes in subtle ways, and the effects of inhomogeneities might have to be considered in more refined treatments. However, a more serious problem is likely to be the neglected effect of hydrothermal convection in permeable materials surrounding the magma.

For convenience and in order to specify notation we give some mathematical results for the three one-dimensional models of Figure 7 and for some related two- and three-dimensional cases. The graphical representation of the solutions will be somewhat more complete than is required by the immediate needs of the present discussion. We have found them to be a useful guide to intuition in problems relating to Long Valley and similar thermal areas. The relations are expressed in terms of conduction length $l(t)$ (Table 2) rather than the time t, so that all of the independent variables have the same dimensions.

For model I the anomalous heat flow $Q(l)$ on the ground surface $z = 0$ above the magma chamber is given at any time by [see, e.g., *Uyeda and Horai*, 1964; *Carslaw and Jaeger*, 1959, p. 313]

$$Q(l)/Q_0 = \left[1 + 2\sum_{1}^{\infty}(-1)^n \exp\left(\frac{-n^2\pi^2 l^2}{4a^2}\right)\right] \tag{4}$$

$$n = 0, 1, 2, \cdots$$

It is represented by the dashed curve in Figure 10a.

For model II the anomalous temperature $\Theta(l, z)$ at any time and depth is given by [*Carslaw and Jaeger*, 1959, p. 62]

$$\frac{1}{\Theta_0}\Theta(l, z) = \frac{1}{2}\left[\operatorname{erf}\frac{\Delta + a - z}{l} - \operatorname{erf}\frac{\Delta + a + z}{l} - \operatorname{erf}\frac{a - z}{l} + \operatorname{erf}\frac{a + z}{l}\right] \tag{5}$$

The temperature Θ_c at the center of the cooling magma, obtained by setting $z = a + \Delta/2$ in (5), is represented in terms of roof thickness a in Figure 8b and in terms of magma thickness Δ in Figure 8a. This is a convenient measure of the temperature in the deep interior of a cooling magma, although the actual depth of maximum temperature will be displaced downward somewhat depending upon the roof thickness a and the vertical gradient in the undisturbed country rock. The vertical dashed line in Figure 7b is a more realistic representation of the initial magma temperature for instantaneous intrusion; the excess temperature Θ_0 will have to be adjusted accordingly in applications of model II to the cooling of thick bodies. The anomalous heat flow at the ground surface above the chamber is

TABLE 2. Conduction Length $l \equiv (4\alpha t)^{1/2}$ km

Time t, m.y.	l'	l''	l'''
0.01	0.7	1.0	1.4
0.1	2.2	3.2	4.5
0.3	3.9	5.5	7.8
0.7	6.0	8.4	12
1	7.1	10	14
2	10	14	20
4	14	20	28
10	22	32	45
20	31	45	64
30	39	55	78

For l', $\alpha = 0.004$; for l'', $\alpha = 0.008$; and for l''', $\alpha = 0.012$, where α is thermal diffusivity (in square centimeters per second or 10^{-4} m^2 s^{-1}).

$$\frac{1}{Q_0} Q(l) = \frac{2}{(\pi)^{1/2}} \frac{a}{l} \left\{ \exp\left(-a^2/l^2\right) - \exp\left[-a^2/l^2\left(1 + \frac{\Delta}{a}\right)^2\right] \right\} \tag{6}$$

It is represented graphically in Figure 8c. The maximum surface heat flow cannot exceed $\frac{1}{2}Q_0$ (see Figure 10a); for $\Delta \lesssim a$ the maximum is substantially less, and it probably occurs after the magma has completely solidified (see Figures 8b and c).

These one-dimensional results for model II are easily generalized to the case of initial temperature Θ_0 in a rectangular parallelepiped of thickness Δ beneath a roof of thickness a. The result has been used widely in discussions of cooling igneous bodies [e.g., *Lovering*, 1935; *Van Orstrand*, 1944; *Jaeger*, 1964; *Simmons*, 1967b; *Blackwell and Baag*, 1973]. It is more convenient than the corresponding result for the sphere [*Rikitake*, 1959; *Carslaw and Jaeger*, 1959, p. 257] because the aspect ratios of the chamber can be adjusted, and it is a bit simpler analytically. The three-dimensional results are obtained by multiplying the results for the slab (e.g., (5) and (6)) by an edge effect factor E that depends only on x, y, l, and the horizontal dimensions of the chamber. We consider only the case of a square prism of horizontal width $2m$, which will be referred to as model IIa (Figure 9, inset). The edge effect factor along the vertical plane of symmetry ($y = 0$) is

$$E(x, l, m) = \frac{1}{2} \operatorname{erf} \frac{m}{l} \left[\operatorname{erf} \frac{m}{l}\left(1 - \frac{x}{m}\right) + \operatorname{erf} \frac{m}{l}\left(1 + \frac{x}{m}\right) \right] \tag{7}$$

This result is shown graphically in Figure 9.

Results for model III, a uniform distribution of continuous heat sources on the infinitely extended plane $z = a$, are given in the appendix (equation (A6)). A generalization, model IIIa (Figure 10a, inset), where the sources occur only on the half plane $x' < 0$, $z = a$, is useful for considering edge effects (equations (A4)). The heat flow at the ground surface is represented by the family of curves in Figure 10a; the curve $x'/a = -\infty$ represents model III. By subtracting the result for a second value of x' the effect of a continuous strip source of finite width can be obtained from the figure. Subtracting the result for a second value of time (i.e., l) gives the effect of a continuous source of finite duration.

A generalization of model III in cylindrical coordinates is called model IIIb. As illustrated by the curves in Figure 10b, it represents the heat flow anomaly above the center of a uniform continuous circular source of radius R at depth a. Heat flow above the apex of a pie slice of central angle λ is obtained by multiplying the result for the circle by $\lambda/2\pi$. Results for various finite and infinite regions including the useful sector of a circular annulus (Figure 10b, inset and equation (A5)) can be obtained by combining results from Figure 10b for various values of R and λ. Discussions of models IIIa and IIIb are given in the appendix.

Depth of the Long Valley magma chamber. The geologic inference that Long Valley was a source of silicic volcanism for a period of about 2 m.y. extending virtually to the present has implications for the depth of the associated magmatic system.

If we assume that the magma temperature was 800°C, the roof thickness a was initially 5 km, and the ambient geothermal gradient was 25°C/km, then at the top of the chamber the ambient temperature was initially 125°C, and the excess temperature of the magma was $\Theta_0 \sim 675°$. If the thermal conductivity K of the overlying heated rock and sediments averaged 4.5 mcal/cm s °C, then the equilibrium upward-conducted anomalous flux would be (equation (2))

$$Q_0 \sim 6 \text{ HFU} \tag{8a}$$

$$Q_0 \sim 200 \text{ cal/cm}^2 \text{ yr} \tag{8b}$$

This value could reasonably be adjusted upward to about 10

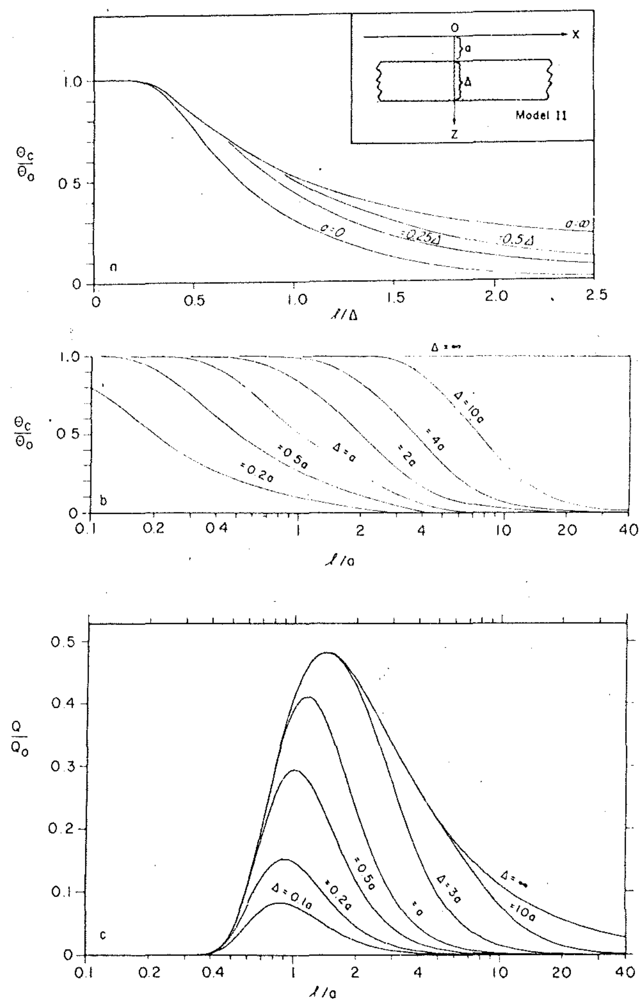

Fig. 8. Model II. The instantaneous slab source with initial temperature excess Θ_0, where l represents 'conduction length' (Table 2): (a) central temperature Θ_c in terms of magma thickness Δ, (b) central temperature Θ_c in terms of roof thickness a, and (c) anomalous surface heat flow Q.

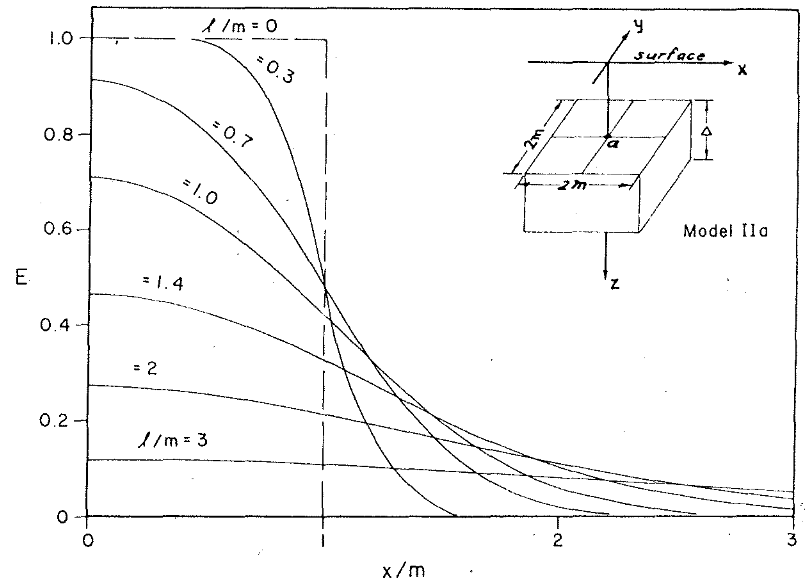

Fig. 9. Model IIa. Edge effect factor E (equation (7)) for heat flow and temperature on the plane $y = 0$ for a square prism. The effect is independent of depth (z).

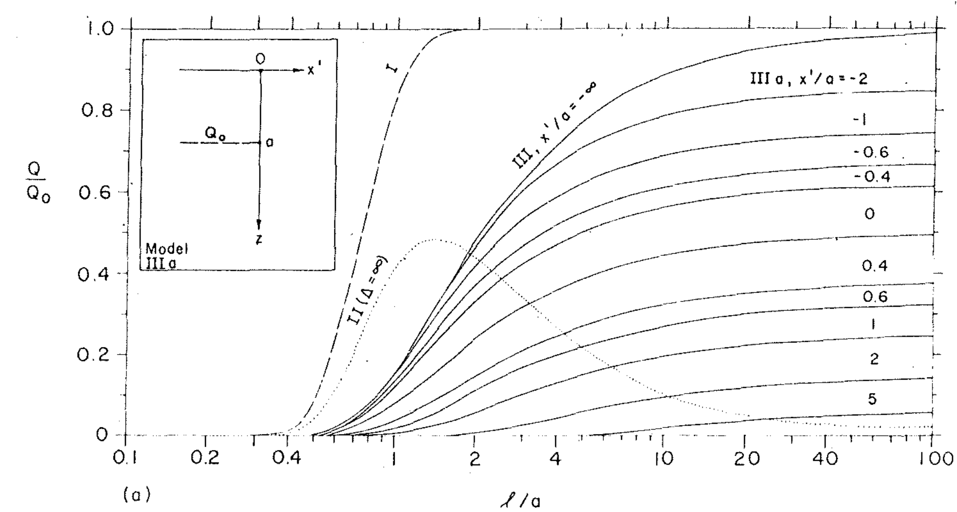

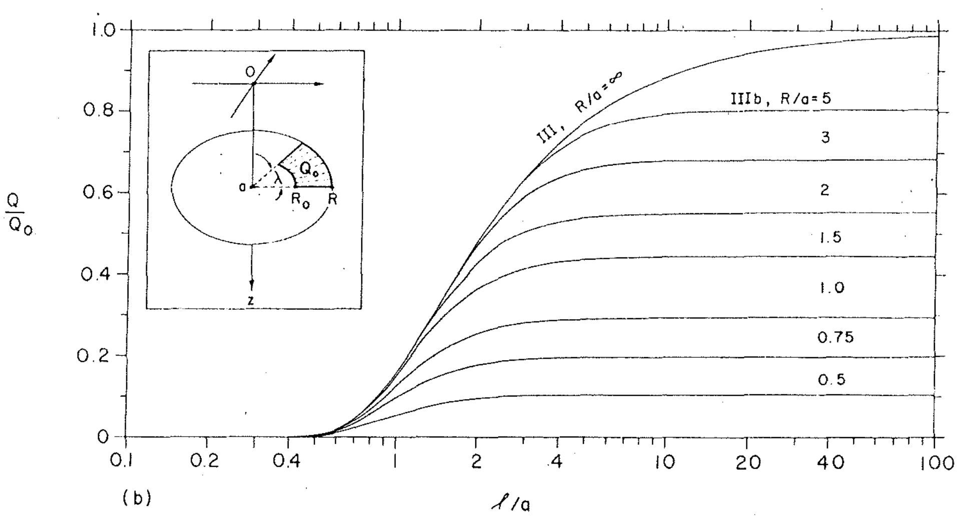

Fig. 10. Surface heat flow from continuous sources of constant strength Q_0 in a region of the horizontal plane $z = a$. (a) Solid curves (model IIIa) represent surface heat flow at x' for sources in the negative half plane (inset). The special case $x'/a = -\infty$ represents model III. Results for model I (dashed curve) and model II, $\Delta = \infty$ (dotted curve), are shown for comparison. (b) Surface heat flow (model IIIb) at origin from sources in the circle $\rho < R$. Inset shows a more general case obtainable by superposition. The special case $R/a = \infty$ represents model III.

HFU or downward to perhaps 4 HFU depending on the assumed ambient temperature, conductivity, and roof thickness. The total heat flow is obtained by adding the regional value, probably $1\frac{1}{2}$–2 HFU. If the latent heat of crystallization of the silicic magma were 65 cal/g [*Harris et al.*, 1970] and the density were 2.5 g/cm^3, crystallization of a layer about 1.2 cm thick each year could supply heat at this rate. Thus heat loss from the upper surface at the rate Q_0 since the start of Long Valley volcanism (~2 m.y. ago) would remove enough heat to crystallize 24 km of silicic magma. If hydrothermal circulation in the roof rocks were appreciable, the heat loss and crystallization rate would have to be increased accordingly [see, e.g., *Lachenbruch et al.*, 1976]. Consider the extreme case in which the Long Valley chamber was a convecting slab of thickness Δ isolated from sources of resupply from below and assume that as crystals formed, they settled, and the roof $z = a$ was continually maintained at 800°C. Neglecting any superheat of the magma, the chamber would have to extend virtually to the base of the crust in order to have been a source of extrusive materials up to the present time. This represents a model like model I (Figure 7) except that the extra heat loss during warming of the roof is neglected; the problem of heat loss during emplacement is, of course, circumvented by the assumed initial condition. If the chamber extended to the base of the crust where the ambient temperature in the Basin and Range province (Figure 4) is not far from the melting curve, the assumption that the chamber was isolated from sources of resupply would not seem reasonable. Thus if the chamber behaved according to this simple extreme, which maximizes heat loss, the duration of extrusive activity at Long Valley would be inconsistent with the view that the chamber was an isolated blister in the upper crust.

We now consider a model that represents slow cooling; it is extreme but not necessarily bracketing. A magma slab of thickness Δ is emplaced at $t = 0$ beneath $z = a$ at a temperature exceeding its surroundings by Θ_0; thereafter it is isolated from its source and cools by homogeneous conduction, inside and outside of the chamber (Figure 7*b*, model II). As gradual accumulation (at excess temperature Θ_0) prior to $t = 0$ would give some of the material a head start in cooling, the initial condition assumed would tend to overestimate the value of t for complete crystallization. The effect of neglecting convection by magma in the isolated cooling chamber and convection by water in fractured roof rocks is also to overestimate the crystallization time. The chief problem is how to cope with the effects of latent heat of crystallization, the theory of which has been discussed in considerable detail by J. C. Jaeger [e.g., *Jaeger*, 1964, 1959, 1961; *Carslaw and Jaeger*, 1959, chap. 11]. He has presented relations that account for contrasting thermal properties of magma, newly crystallized material, and country rock; for latent heat release over a finite melting interval; for intrusion at temperatures above the liquidus; and, to some extent, for geometric irregularities. Each of these effects can significantly influence the crystallization time and the thermal regime within and immediately around the chamber. However, application of these relations is not warranted, as it involves many parameters, most of which have not yet been carefully considered for Long Valley. In any event, results would be uncertain because of neglected effects of hydrothermal circulation. We shall use a scheme contrived to yield very approximate results from inspection of Figures 8 and 9. We suppose that crystallization is complete when the central part of the chamber has cooled by such an amount ($\delta\Theta$, calculated by neglecting latent heat) that the heat withdrawn locally is equivalent to the latent heat. Thus

$$\delta\Theta = (L/c) \sim 215°\text{C} \tag{9}$$

where L is the latent heat, assumed to be 65 cal/g, and c is the specific heat of the magma, assumed to be 0.3 cal/g °C. Hence we shall consider crystallization to be complete when the central temperature Θ_c calculated from model II falls to

$$\Theta_c \sim \Theta_0\left[1 - \frac{L}{c\theta_0}\right] \tag{10a}$$

$$\Theta_c \sim \Theta_0\left[1 - \frac{215°\text{C}}{\theta_0}\right] \tag{10b}$$

The model is most likely to be reasonable if Θ_0 is close to the liquidus temperature and the temperature interval for crystallization is small, as in the case of freezing along the cotectic curve [e.g., *Winkler and Lindemann*, 1972]. In this case the true central temperature at the time of complete crystallization will still be at or near Θ_0, and the central temperature Θ_c used for estimating crystallization time will be 215°C less. If the crystallization interval is large, say 200°C, the model could underestimate the crystallization time. The total heat loss from the magma computed by the approximation will generally be somewhat less than the true heat loss during complete crystallization, but the crystallization time will be overestimated by it for many cases of practical interest. This is possible because latent heat has two opposing effects on the cooling of a chamber: it increases the amount of heat that must be removed, but it also increases the rate at which heat is lost.

Figure 8*a* shows that as long as the magma thickness is greater than the conduction length ($l/\Delta \lesssim 1$) and is not greater than twice the roof thickness ($a > 0.5\Delta$), proximity to the earth's surface does not affect the decay of the central temperature. In this case (by symmetry) we can identify Θ_0 with the excess temperature at the level of the midpoint of the intrusive ($z = a + \frac{1}{2}\Delta$). For an 800°C magma with its midpoint at the 10-km depth in a region with an undisturbed gradient of 25°C/km, we obtain $\Theta_0 = 550$°C. Equation (10*b*) then gives $\Theta_c/\Theta_0 \sim 0.6$, and according to Figure 8*a*, crystallization is essentially complete when $l/\Delta \sim 0.8$. Choosing the lowest value of α in Table 2 as a conservative estimate of properties in the magma, we find for a 0.7-m.y.-old chamber that $l' \sim 6$ km and consequently $\Delta \sim 7\frac{1}{2}$ km. Thus a $7\frac{1}{2}$-km-thick magma that intruded beneath a 6-km roof at the time of eruption of the Bishop Tuff could not be a volcanic source today. If the intrusion had accumulated over some finite period prior to 0.7 m.y. ago, it would, of course, have solidified at some time before present. Crystallization would occur earlier also if, as seems likely, the chamber included portions of solid country rock or was partially crystallized at the time of intrusion; in that case, L and $\delta\Theta$ (equation (9)) would be overestimated. A less conservative estimate of properties (using α'' instead of α'; Table 2) would have led to crystallization of an intrusion 10 km thick beneath a 5-km roof for the same conditions.

More massive intrusions for which the present approximation is less satisfactory would, of course, be required to survive the 2-m.y. volcanic history at Long Valley without resupply from a deeper source. For such large values of time an appreciable amount of cooling takes place from the edges of the chamber. Taking $m = 10$ km in Figure 9 to approximate conditions at Long Valley, the appropriate horizontal temperature profiles through 1- and 2-m.y.-old prisms are given by the curves $l'/m = 0.7$ and 1.0, respectively (Figure

9 and Table 2). Hence the central temperature in the prism (at $z = a + \frac{1}{2}\Delta$, $x = y = 0$) is 90% of that in the slab after 1 m.y. and 70% after 2 m.y. These differences would substantially reduce one-dimensional estimates of crystallization time and further increase the initial thickness required for survival of melt in an intrusive chamber isolated from sources of resupply.

These results taken collectively suggest that an independent intrusive chamber with lateral dimensions of Long Valley caldera and a thickness up to perhaps 10 km would be crystallized by conductive heat loss no more than 1 m.y. or so after its magma supply was cut off. If the magma convected or if hydrothermal loss were appreciable, the time would be substantially less. The result is relatively insensitive to the thickness of the roof (for a given temperature contrast). For times longer than 1 m.y. the edge losses become substantial, and an uppercrustal silicic magma chamber probably could not sustain molten material as required by the geologic observations, unless it were repeatedly resupplied with heat from deep-crustal or subcrustal magmatic sources.

Present state of the Long Valley magma chamber. Judging from estimates of structural collapse and volumes of material removed during eruption of the Bishop Tuff [*Bailey et al.*, 1976], the entire area of the caldera was probably underlain by a magma layer at least 1 or 2 km deep for some unknown period prior to the eruption 0.7 m.y. ago. The resurgent structure forming shortly thereafter (0.6 m.y. ago) indicates a roof thickness of perhaps 5–7 km at that time. Recent volcanism [*Bailey et al.*, 1976] implies that a source of silicic magma probably still exists in the chamber today, at least in the western part. The question arises whether shallow molten material could still underlie the entire region occupied by the caldera. If heat transfer were primarily by conduction, surface heat flow measurements should provide a definitive answer. However, hydrothermal circulation precludes the application of heat conduction theory to measurements within the caldera [*Lachenbruch et al.*, 1976], and conductive heat flow measured in the surrounding rocks could be affected even if circulation were confined to the caldera proper. Effects of hydrothermal convection within the caldera on conductive flux beyond its rim could be of either sign depending upon details of the circulation. As these details are unknown, we shall neglect them and consider the present thermal state in terms of simple conduction models. Although this assumption renders the conclusions uncertain, the analysis provides a useful frame of reference.

We know from model III (Figure 7*c*) that if heat is released at some depth a in a nonconvecting solid at an average rate Q_0 (equation (2)), after an infinite amount of time the excess temperature there will reach Θ_0, the value required for a stable magma chamber. Thus if the average rate of heat release is greater than Q_0, a chamber will ultimately develop, and if it is less, a chamber will not develop. The quantity Q_0 is smaller at greater depth, both because a is larger and because Θ_0 is smaller (equation (2)). Hence it is generally easier to develop a stable magma chamber at greater depth. We might view the heat release Q_0 as the result of successive intrusion and crystallization at depth a of thin sills with a thickness $\Delta << a$. How the sensible and latent heat is conducted and convected away from a real sill depends upon the mechanics of intrusion and upon hydrologic conditions in the surrounding rock. In any case, solidification of a 1-meter sill every century would release latent heat at the average rate of about 7 HFU; in the early stages when the country rock was cool, sensible heat would be released at a comparable rate. Hence average intrusion rates of at least 1 m every century or so would probably be required to develop a stable chamber at the 5-km depth; at the 10-km depth the required rates would be roughly half as great. Where circulating water removes appreciable heat, estimates of Q_0 and intrusion rates must be increased accordingly. Sills that were fed at rates much greater than these minima might be expected to develop quickly into viable magma chambers; if their upper surfaces were kept in contact with magma by convection, temperatures above them would be represented by model I (Figure 7*a*). Comparison of the gradient at $z = a$ for the curves labeled t_1 in models I and III (Figure 7) shows that the upward heat loss is much greater from the early developing chamber; this, of course, is why the surface heat flow grows to the equilibrium value Q_0 much faster in model I than in model III (Figure 10*a*, curves I and III).

From the foregoing we expect model III to provide a lower limit to the surface heat flow above a developing or established magma chamber at depth a for the case of one-dimensional conductive transfer. The model has the advantage of being easily modified to consider heat flow across the edge of sources of limited lateral extent (models III*a* and III*b*). We assume that the limited source models apply at and beyond the rim of Long Valley caldera; whether the assumption is justified depends upon unknown effects of hydrothermal circulation. For a 1-m.y.-old chamber at the depth $a = 5$ km we have $l''/a = 2$ (Table 2). Coincidence of the curves $R/a = 3$ and $R/a = \infty$ for $l/a \lesssim 2$ (Figure 10*b*) indicates that sources whose lateral distances from the heat flow station exceed 15 km will not contribute appreciably. Therefore for this example the magma sheet beneath the caldera can be represented by the semi-infinite region of model III*a* (Figure 10*a*). The position $x' = 0$ might be identified with the heat flow site WC on the eastern rim of the caldera, and Watterson Trough (WTE) and Round Mountain (RM) would correspond, respectively, to $x' = 3$ km and $x' = 6$ km (Table 1). For $a = 5$ km this model leads to heat flow anomalies at these sites of 1.4, 0.7, and 0.3 HFU, respectively. If the chamber had been developing under this region for the past 2 m.y., these values would be larger by 30–50%, and if it existed only for the past 0.7 m.y., they would be smaller by only 10–20%. Figure 5 and Table 1 show that no such anomalies are indicated at these sites if the Basin and Range norm applies for them. If the magma surface were represented (less conservatively) as a region of constant temperature at depth a, the edge effects would develop much more rapidly, and the predicted heat flow anomalies would be even larger. (Steady state results for the constant temperature case can be estimated from model III*b*; see appendix.) Although the model is uncertain chiefly because of neglected hydrothermal effects, it suggests that the measured heat flow is inconsistent with the continuous existence of magma only 5 km beneath the eastern portion of the Long Valley caldera throughout its recent eruptive history. A similar conclusion is probably justified for magma at a depth of 7 km. However, magma at the 10-km depth leads to substantially smaller anomalies and probably cannot be ruled out on present evidence by this model.

We now consider what magmatic history for the eastern caldera is consistent with the conditions that shallow magma occurred there 0.7 m.y. ago and that heat flow near the eastern rim is normal or nearly so today. The conduction time constant for a 5- to 7-km roof (i.e., the value of t for $l'' \sim 5$–7 km; Table 2) is less than 0.7 m.y.; hence substantial cooling could have occurred by conduction alone in the eastern caldera if the heat sources beneath it were removed with eruption of the

Bishop Tuff. Extension of the foregoing constant source model indicates that if a chamber developed 5–7 km beneath the eastern half of the caldera about 1 m.y. ago and was evacuated 0.3 m.y. later, a heat flow anomaly probably would not be detectable near the eastern rim today. A constant temperature conduction model of the magma would imply that the molten condition beneath the eastern rim was of shorter duration or possibly that the residual magma there was quenched by hydrothermal convection. In any case, it seems consistent to speculate that eruption of the Bishop Tuff may have largely exhausted the magma in the eastern part of the caldera, leaving a residual magma chamber more circular in plan under the western part of the caldera. By this view the asymmetric position of the resurgent dome would mark the location of this hypothetical residual chamber. These suggestions are speculative because of the unknown role of hydrothermal convection and the preliminary status of the heat flow data. Curve I (Figure 10*a*) shows that the absence of a heat flow anomaly does not preclude a more recent intrusion beneath the eastern part of the caldera, say, in the last 0.1 and 0.2 m.y. ($l''/a \lesssim 1/2$), although there is no present evidence that this has occurred.

The foregoing discussion depends upon the nearly normal heat flow to the east to tell us where the magma could not have been and upon geologic observations to tell us where it must have been. Inside the Long Valley caldera the thermal regime is strongly influenced by water movements [*Lachenbruch et al.*, 1976], and outside of it we have only one observation of an anomalously large heat flow, the site DP about 3 km beyond the western rim. This anomaly of 2.75 HFU could be the effect of a still molten, geometrically simple Long Valley magma chamber. If it is, a model of the type just discussed would suggest that the roof of the chamber is not deep (perhaps about 5 km) and that the chamber might even extend a few kilometers beyond the western caldera rim. It is interesting that at Valles caldera, New Mexico, whose size and recent eruptive history are rather similar to Long Valley's, a site similar to DP (3 km west of the rim in granitic rock) also yields a heat flow of 3.5–4.0 HFU [*Potter*, 1973]. This observation might lend some support to the foregoing simple explanation. Alternatively, the high value at DP might be a local effect of the extensive recent magmatic activity along the Sierra Nevada frontal fault system in the vicinity of Devils Postpile. If the second alternative is true, the observation at DP contains no information on the present state of the Long Valley magma chamber, and the best evidence for existence of a chamber is the very recent silicic extrusion attributed to it [*Bailey et al.*, 1976] and perhaps the hydrochemical estimates of large heat flux from the caldera [*White*, 1965; *Sorey et al.*, 1976; *Lachenbruch et al.*, 1976]. Additional heat flow measurements near the western rim of the caldera could provide a basis for selection between these alternatives.

Background heat flow near the province boundary and the measurement at AB. The foregoing examples illustrate how simple heat conduction models can be used with heat flow measurements near a volcanic area to guide speculation on the magmatic history and the present thermal state. Ignorance of the geometric distribution of thermal properties and of convective movements (both magmatic and hydrologic) throughout this history will often preclude the useful application of elaborate analytical or numerical thermal models, even if the distribution of heat flow in the vicinity is very well known. If the distribution of heat flow is not well known, as in the Long Valley study at its present stage, the implications of even the simple extreme models (e.g., Figures 8, 9, and 10) can be uncertain. This uncertainty has been illustrated by the foregoing discussion and particularly by the example of the single measurement DP near the west rim of the caldera. It is illustrated in another way by the measurement at Aeolian Butte and its bearing on the interpretation of the province transition and heat flow at the east rim sites.

The inference that heat flow is normal or nearly so near the east rim of the caldera is based on the supposition that the Basin and Range norm applies approximately to the background heat flow there. Under that condition the measured anomaly at the rim and at distances of 3 and 6 km beyond it would be +0.4, −0.2, and −0.3 HFU, respectively (Q_{BR} for WC, WTE, and RM, Table 1). We have pointed out that such variations from the norm are typical of sites interior to the Basin and Range province where there is no obvious association with very recent volcanism. The sites in question, however, lie an average of perhaps 15 or 20 km from the boundary of the Sierra Nevada physiographic province. It might be argued that the typical Basin and Range values measured near the east rim are a coincidence resulting from canceling effects of a regional transition to the lower heat flow characteristic of the Sierra and the anomalous heat from the Long Valley magma chamber. If we took the extreme position that the Sierra norm applied at the east rim, the anomalies there (Table 1, Q_S) would be larger by 1 HFU, and the effects of magmatic heat would be judged significant. However, there is no observational evidence to support this position. Apart from the measurement at JM and SM, which are probably controlled by hydrologic effects, we have two other measurements (DS and AB, Figures 1, 2, and 5) in granitic rocks of the Basin and Range province in the area. Both are too far from the caldera to be affected by it, and both yield data consistent with the Basin and Range norm. One site (DS) is about 10 km farther from the physiographic province boundary than the east rim, and the other (AB) is about 10 km closer to it. Although the normal Basin and Range value at AB (less than 10 km from the province boundary) deepens the puzzle of the province transition, it tends to confirm the validity of the Basin and Range norm at the east rim of the caldera.

Aeolian Butte is probably closer to the physiographic boundary than any other site yielding normal Basin and Range heat flow. The measured heat flow and heat production there are well-established values at a location in the center of a Mesozoic pluton. However, the site also lies in the center of *Kistler*'s [1966] ring fracture zone (Figure 2), which contains areas of very recent volcanism, including the Mono craters on its eastern rim. *Bailey et al.* [1976] have suggested that the ring fracture zone is probably underlain by a modern magma chamber. Thus we could speculate that the normal heat flow at AB is transitional and that AB falls on the Basin and Range curve by coincidence because of an anomaly from the hypothetical crustal magma source, a problem similar to that on the east rim of Long Valley.

We should like to know whether such a chamber exists, both as a matter of geologic interest and because of its bearing on the interpretation of background heat flow in the Long Valley area. With only one measurement near the ring fracture zone it is difficult to resolve this question, but if we assume it to be representative, some information can be obtained.

According to *Kistler* [1966, p. E48], faulting on the ring fracture occurred after the Sherwin glaciation (minimum age ~1 m.y. [*Dalrymple*, 1964]) and before the eruption of the Bishop Tuff 0.7 m.y. ago [*Bailey et al.*, 1976]. (More recent displacements have also occurred on some parts of the fracture zone (R. A. Bailey, personal communication, 1975).) If the activity on the ring fracture is a mechanical effect of the hypothetical magma chamber beneath it, the chamber must be at least 0.7 m.y. old, and according to Table 2, $l'' \geq 8.4$ km and $l''' \gtrsim 12$ km; the most reasonable value in this case is probably closer to l'''. The radius of the ring fracture zone is about 6 km. If it were underlain by magma at a depth of 6 km, then by model III*b* the heat flow anomaly at AB would be $\gtrsim 0.25\ Q_0$ (Figure 10*b*, $R/a = 1$, $l/a \gtrsim 2$), i.e., probably greater than $1\frac{1}{2}$ HFU in these crystalline rocks ($K \sim 6$ CU). But even if AB were interpreted in terms of the Sierra norm, the measured anomaly at AB would not exceed 0.9 HFU (Table 1, Q_S), and a more reasonable interpretation of the province transition would limit the anomaly further. Extension of the argument suggests that if a stationary chamber exists beneath the ring fracture, its roof is probably at least 8–10 km deep; it could be shallower if it had changed its position rapidly in recent times. If such a chamber supplied the very recent volcanism in the area, it probably did so along deep local conduits. Additional measurements of heat flow in this region might provide useful information on the nature of the local magmatic system and the province transition.

THERMAL IMPLICATIONS FOR MASS TRANSFER AND CRUSTAL SPREADING

It is unlikely that silicic melt can be maintained in the upper 5–8 km of the crust for periods of the order of a few million years without anomalous upward heat loss at the average rate of at least 5–10 HFU; this estimate allows little for hydrothermal circulation in the roof rocks. We suppose that this minimum condition obtained in those places with lateral dimensions of a few tens of kilometers where silicic volcanism was associated with caldera formation [*Smith and Bailey*, 1968]. If conductive transfer predominates, this thermal anomaly might not appear at the surface for several hundred thousand years; if hydrothermal convection occurs, the anomaly could be much larger, and it might never appear in the conductive flux at the earth's surface above the melt, as the heat could be discharged by hot springs. The Basin and Range crust is 30 km or so thick [*Thompson and Burke*, 1974], and hence 5–10 HFU cannot be transferred through it by conduction without prohibitively large subcrustal temperatures [*Blackwell*, 1969, 1971]. Therefore the large heat flux implies vertical transfer of mass through the crust; to maintain the molten condition the mass must deliver heat to the melt at temperatures at or above 800°C or so.

Christiansen and Lipman [1972] document the universal association of basalts with rhyolitic volcanism in the Basin and Range province and propose that the 'basalts represent the fundamental expression of deep-seated processes and that the rhyolites are directly related to the rise of basaltic magmas in the earth's crust.' This seems plausible as the high melting temperature, large latent heat, and low viscosity of basalt [*Shaw*, 1965; *Shaw et al.*, 1968] make it a most effective heat transfer fluid for crustal magmatic processes. Furthermore, temperatures represented by the Basin and Range norm (Figure 4) are consistent with the existence of basaltic melt at or slightly below the base of the crust [see also *Roy and Blackwell*, 1966; *Roy et al.*, 1972; *Blackwell*, 1971; *Archambeau et al.*, 1969; *Pakiser and Zietz*, 1965].

Basaltic sills (with latent heat of 100 cal/g, density of 3 g/cm^3, and specific heat of 0.3 cal/g °C) intruding the crust at 1100°C and then crystallizing and cooling to 800°C at average rates of 1 cm/yr would supply heat at the rate of about 18 HFU. (The intrusions could, of course, be of any geometric form; we mention sills to emphasize that the calculation is one-dimensional.) Presumably their heat could mobilize or melt in place indigenous silicic material to produce the laterally extensive upper crustal melts implied by caldera collapse. Whether the basalt transferred its heat to the upper crustal melt by inducing convection in a deep silicic magma chamber, by melting silicic rock which ascended to replenish upper crustal sills, or by direct intrusion of the upper crust to rejuvenate crystallizing melt, only the heat available in the basalt above 800°C or so could contribute to the upward heat loss as required to preserve the upper crustal melt. To supply the estimated minimum heat loss from the top of the silicic melt for 2 m.y. by these processes would require the local addition to the crust (beneath the top of the melt) of a layer of basalt on the order of 10 km thick. (The requirement would be even greater if we allowed for heat lost to lower crustal rocks at temperatures below 800°C.) This would result in substantial crustal thickening unless the original crustal material were displaced downward into the mantle or sideways by local crustal spreading.

Simple calculations are possible if we assume somewhat arbitrarily that basaltic additions necessary to supply the excess heat are accommodated by local crustal spreading with little change in crustal thickness and that convective input from below and surface heat loss have achieved a steady state. In this case the anomalous heat flux and the local spreading strain rate are proportional to one another (as both are proportional to the upward flux of basalt). Such a process could be consistent with the model of *Thompson and Burke* [1974] in which passive basaltic dikes fill extension fractures at the base of the laterally spreading Basin and Range crust. In an area of active silicic volcanism, basaltic intrusion would be intense, and the locally weakened crust might relieve regional tectonic strain at an accelerated rate. This model would suggest that subcrustal intrusion and volcanism might cease after the accumulated regional strain is relieved locally. For a 30 km crust and the conditions assumed above, crustal area would increase at the rate of about 2% per million years per anomalous HFU. Thus anomalous heat loss of 5–10 HFU from the top of the Long Valley magma chamber for 2 m.y. would be associated with an area increase on the order of 20–40%, e.g., extension of a 25-km square by 5–10 km in one direction.

A similar calculation can be applied to the Basin and Range province as a whole if we assume that the excess regional flux is provided by distributed basaltic intrusions in the lower crust, cooling to the reasonable ambient temperature of 800°C (Figure 4). Although it is still uncertain, the anomaly in the flux (equation (1), q^*) from the lower crust of the Basin and Range province is estimated to be about 0.6 HFU relative to stable continental regions [*Roy et al.*, 1968]. If this anomalous thermal condition has persisted throughout the 15-m.y. history of the structural province, the foregoing model leads to an increase in its average area of about 20%. This would represent a total E-W extension throughout the life of the Basin and Range province of 150–200 km and a mean spreading rate of the order of 1 cm/yr. These tenuous results are within the range of values estimated by other means [*Thompson and Burke*, 1974].

Because of the likelihood of basaltic melt at or slightly below the base of typical Basin and Range crust, the Basin and Range heat flow 'norm' is, in a sense, a magmatic thermal anomaly. Near the edge of the province (e.g., in the Long

Valley area) the problem of distinguishing between the effects of the province transition and those of upper crustal magmatism is that of distinguishing between a deep magmatic anomaly and a shallow one. General availability of basaltic melt in the subcrust of the Basin and Range would make both types of anomalies likely, and this probably contributes to much of the variability of heat flow in the province. Curve I, Figure 10*a*, and Table 2 show that 'normal' Basin and Range heat flow would probably obtain no more than 5 or 10 m.y. after basaltic melt becomes established in the subcrustal region; if the formation of Basin and Range crust were initiated by silicic volcanism, the thermal 'norm' could be established faster. Development of the thermal edge effect by conduction in the deep-rooted crust of the adjacent Sierra Nevada province is a longer process. Thus the abrupt thermal transition across the province boundary might imply a westward encroachment of the Basin and Range province on the Sierra Nevada province in the last several million years [see also *Roy et al.*, 1972]. Unfortunately, the heat flow data near the province boundary are not yet adequate for an analytical discussion of this problem.

SUMMARY

Heat flow was measured at 11 sites in the vicinity of Long Valley caldera in a search for information on the local magmatic history and present thermal state. The problem is complicated by hydrothermal convection and by the location of Long Valley astride the boundary between the Sierra Nevada and Basin and Range physiographic provinces, the locus of one of the sharpest transitions in regional heat flow in North America. The locations of the new sites range 30 km or so on either side of the province boundary and 0–30 km (outward) from the caldera rim. Four previously published values from the Sierra Nevada and one from the Basin and Range extend the regional coverage. With three notable exceptions (two of which are attributed to moving groundwater) the values of heat flow and heat production are within the range expected at points interior to each province. Hence individual effects of either the province transition or of recent magmatic heat are not generally conspicuous. As these effects are of opposite sign in the Basin and Range, there is, of course, the possibility that they both occur and are self-canceling. Four measurements near the eastern rim of the caldera indicate that if an anomaly (relative to the Basin and Range norm) exists there, it is very local and probably not greater than a few tenths of a heat flow unit. An important exception to the normal pattern is the single value measured near the western rim where the anomaly is 2.75 HFU in relation to the Sierra norm. Although the new data are preliminary and their geographic distribution is sparse, it is useful to use them with simple heat conduction models and geologic information to explore possible constraints on the magmatic regime and to identify areas where additional observations might be most helpful.

According to *Bailey et al.* [1976] the region beneath Long Valley has been the source of silicic volcanic material over a period beginning about 2 m.y. ago and extending virtually up to the present. Simple heat conduction models suggest that such a source probably could not have survived crystallization unless it was resupplied with heat from deep crustal or subcrustal magmatic sources. In this sense, Long Valley caldera represents the surface expression of a deep magmatic system.

It seems likely that the heat supply at some stage involves the movement of basalt [*Christiansen and Lipman*, 1972], the most effective heat transfer fluid for crustal magmatic processes [*Shaw*, 1965; *Shaw et al.*, 1968]. This suggests an idealized model (following *Thompson* [1966]) in which mantle basalts replenish the spreading crust by intruding tensile openings in its base. They supply the anomalous heat loss which would therefore be proportional to local spreading strain rate if a steady state is approached. For the special conditions assumed in the text this leads to crustal extension of the order of 2% per million years per anomalous HFU; for a province-wide anomaly of 0.6 HFU this yields an average spreading rate across the Basin and Range province of the order of 1 cm/yr. In regions of active silicic volcanism the anomalous heat loss is an order of magnitude greater than the anomalous regional flux and by this simple model, so is the local rate of basaltic intrusion and crustal extension.

Judging from the collapse and resurgence following eruption of the Bishop Tuff, the Long Valley caldera was probably underlain by silicic magma at a depth of perhaps 5–7 km about 0.7 m.y. ago [*Bailey et al.*, 1976]. If magma had persisted at such depths throughout the recent eruptive history of Long Valley, we should expect a more conspicuous heat flow anomaly near the eastern rim than we infer from the observations. The time constant for decay of such an anomaly is a few hundred thousand years. Hence we speculate that eruption of the Bishop Tuff exhausted the magma source beneath the eastern caldera and that the subsequent resurgence in the western part identifies the position of a residual chamber, more circular in plan. This interpretation is consistent with the absence of silicic extrusion in the last 0.3 m.y. on the eastern side of the resurgent structure. A source of uncertainty in the interpretation is the unknown effect of hydrothermal circulation beneath the caldera. The high heat flow near the western rim can be interpreted in terms of a simple shallow magma chamber, possibly extending a bit beyond the caldera rim, or perhaps it is a local effect of recent magmatic activity along the Sierra frontal fault system. Additional heat flow measurements could help resolve this ambiguity.

Bailey et al. [1976] have suggested that a modern magma chamber underlies the ring fracture zone associated with Mono craters, about 15 km northwest of the Long Valley caldera. A geologic constraint on the age of the ring fracture and a heat flow measurement at its center imply that if a stationary chamber exists there, its roof is probably deeper than 8–10 km.

The general significance of an individual heat flow measurement is always uncertain, and the sparse distribution of observations in the Long Valley area together with incompletely understood hydrothermal effects leaves fundamental thermal questions subject to more than one plausible answer. However, this preliminary study suggests that investigation of heat flow can yield information not obtainable in other ways about the magmatic system at Long Valley and similar thermal areas.

APPENDIX: THE HEAT FLOW ANOMALY CAUSED BY CONTINUOUS SOURCES IN A FINITE REGION OF A BURIED HORIZONTAL PLANE

We wish to find expressions for the heat flow $Q(x, y, 0, t)$ at the surface, $z = 0$, when the region $z > 0$ is initially at zero temperature under the following condition: heat is generated at the constant rate Q_0 cal/cm² s in the region $(S: x', y', a)$ of the plane $z = a > 0$ for $t > 0$ while the surface $z = 0$ is maintained at zero temperature.

The contribution to the gradient at time t at a point $(x, y, 0)$ on the surface $z = 0$ due to a unit instantaneous heat source at (x', y', a) liberated at time τ is given by [*Carslaw and Jaeger*, 1959, p. 370]

$$\frac{a}{8K(\pi\alpha)^{3/2}}(t-\tau)^{-5/2}\exp\left[\frac{-r^2}{4\alpha(t-\tau)}\right] \quad \text{(A1)}$$

where $r^2 = (x-x')^2 + (y-y')^2 + a^2$. We can therefore express the solution to the problem as follows:

$$\frac{1}{Q_0}Q(x, y, 0, t) = \frac{a}{8(\pi\alpha)^{3/2}}\int_0^t \iint_S (t-\tau)^{-5/2} \cdot \exp\left[\frac{-r^2}{4\alpha(t-\tau)}\right] d\tau\, dx'\, dy' \quad \text{(A2)}$$

We now consider a second problem. Find the temperature $T(x, y, a, t)$ at depth $z = a$ in the region $z > 0$ initially at zero temperature under the following condition: the region (S: x', y', 0) of the surface $z = 0$ is maintained at constant temperature T_0 for $t > 0$ while the rest of the surface $z = 0$ is maintained at zero temperature. It will be seen from the Green's function formulation of this problem [e.g., *Carslaw and Jaeger*, 1959, p. 371; *Birch*, 1950, equation (3); *Lachenbruch*, 1957*b*, equation (23)] that the solution is identical to (A2) if we replace Q by T and Q_0 by T_0. Thus for these two seemingly unrelated problems, we have the following: The temperature disturbance at (x, y, a, t) due to a uniform anomalous temperature in the region (S: x', y', 0) on $z = 0$ for $t > 0$ is the same as the heat flow disturbance at $(x, y, 0, t)$ due to a uniform continuous heat source distribution in the region (S: x', y', a) on $z = a$ for $t > 0$. The region is initially at zero temperature, and the surface temperature is zero except where otherwise specified.

Therefore results for the corresponding temperature anomaly problem can be applied to this problem of anomalous continuous sources.

Integration with respect to time in (A2) yields the general result

$$\frac{1}{Q_0}Q = \frac{1}{2\pi}\iint_S \left[\frac{2}{(\pi)^{1/2}}\frac{r}{l}\exp(-r^2/l^2) - \operatorname{erfc}\frac{r}{l}\right] d\Omega \quad \text{(A3}a\text{)}$$

$$\frac{1}{Q_0}Q \rightarrow \frac{1}{2\pi}\Omega(x, y; S) \qquad t \rightarrow \infty \quad \text{(A3}b\text{)}$$

where $d\Omega$ is the element of solid angle subtended by the surface element $dx'\,dy'$ in S at the field point $(x, y, 0)$ and Ω is the solid angle subtended by S there. Equation (A3*b*) is the well-known result from potential theory, widely used in the interpretation of gravity anomalies [see, e.g., *Nettleton*, 1942; *Simmons*, 1967*a*]. Equation (A3*a*) generalizes the result for transient heat conduction. The integrand is a simple time-dependent weighting factor, and the integral is easily evaluated numerically. (Related results have been obtained by *Birch* [1950].) The continuous source case for which S is the half plane $z = a$, $x' < 0$, has been solved for the corresponding anomalous boundary-temperature problem [*Lachenbruch*, 1957*a*, equation (5)]

$$\frac{1}{Q_0}Q(x, a, l) = \frac{1}{2}\operatorname{erfc}\frac{a}{l} - \frac{1}{\pi}\int_0^{x/a}\exp\left[-\frac{a}{l}(1+\beta^2)\right]\frac{d\beta}{1+\beta^2} \quad \text{(A4}a\text{)}$$

$$\frac{1}{Q_0}Q \rightarrow \frac{1}{2} - \frac{1}{\pi}\tan^{-1}\frac{x}{a} \qquad t \rightarrow \infty \quad \text{(A4}b\text{)}$$

Equations (A4*a*) and (A4*b*) represent model III*a* illustrated in Figure 10*a*. (There we have replaced x by x' to avoid confusion with the notation for model II*a*.) The integral in (A4*a*) has been tabulated [*Lachenbruch*, 1957*a*; *Smith*, 1953].

The corresponding problem in cylindrical coordinates (ρ, ϕ, z) has also been considered for the anomalous boundary-temperature case [*Lachenbruch*, 1957*b*]. The surface heat flow at $z = 0$, $\rho = 0$, due to a continuous uniform source distribution of strength Q_0 for $t > 0$ at depth $z = a$ in the region $R_0 < \rho < R$, $0 < \phi < \lambda$, is [*Lachenbruch*, 1957*b*, equation (33)]

$$\frac{Q}{Q_0} = \frac{\lambda}{2\pi}\left\{\left[1+\left(\frac{R_0}{a}\right)^2\right]^{-1/2}\operatorname{erfc}\frac{a}{l}\left[1+\left(\frac{R_0}{a}\right)^2\right]^{1/2} - \left[1+\left(\frac{R}{a}\right)^2\right]^{-1/2}\operatorname{erfc}\frac{a}{l}\left[1+\left(\frac{R}{a}\right)^2\right]^{1/2}\right\} \quad \text{(A5)}$$

The geometric conditions for this result are illustrated by the inset in Figure 10*b*. The result for the circular region ($R_0 = 0$, $\lambda = 2\pi$) is shown graphically in Figure 10*b* as model III*b*. The circle of infinite radius ($R \rightarrow \infty$), of course, represents the one-dimensional case, model III.

$$Q/Q_0 = \operatorname{erfc}\frac{a}{l} \quad \text{(A6)}$$

The steady state result ($l \rightarrow \infty$) is obtained by setting the complementary error functions to unity in (A5) and (A6). It can be used as an approximation (and lower limit) to the steady state heat flow above a horizontal plane region at constant temperature Θ_0 (equation (2)). The steady state is approached much faster above a constant temperature region than above a constant source region (e.g., compare curves I and III, Figure 10*a*).

Transient effects of continuous or intermittent sources in certain regions bounded by lines of the polar and Cartesian coordinate systems can be obtained by combining (A4) and (A5).

Acknowledgments. We are grateful to Carl Bunker for measurements of the content of U, Th, and K in our rock samples and to D. E. White, R. L. Christiansen, P. C. Bateman, G. B. Dalrymple, R. W. Kistler, R. A. Bailey, and S. P. Galanis, Jr., for helpful discussions. We also thank D. E. White, R. A. Bailey, D. D. Blackwell, W. H. Diment, D. L. Williams, Mary O'Neill, L. J. P. Muffler, and Gene Simmons for comments on the manuscript.

REFERENCES

Archambeau, C. B., E. A. Flinn, and D. G. Lambert, Fine structure of the upper mantle, *J. Geophys. Res.*, *74*, 5825–5865, 1969.

Bailey, R. A., G. B. Dalrymple, and M. A. Lanphere, Volcanism, structure, and geochronology of Long Valley caldera, Mono County, California, *J. Geophys. Res.*, *81*, this issue, 1976.

Bateman, P. C., and J. P. Eaton, Sierra Nevada batholith, *Science*, *158*, 1407–1417, 1967.

Birch, F., Flow of heat in the Front Range, Colorado, *Geol. Soc. Amer. Bull.*, *61*, 567–630, 1950.

Birch, F., R. F. Roy, and E. R. Decker, Heat flow and thermal history in New England and New York, in *Studies of Appalachian Geology: Northern and Maritime*, edited by E. Zen, W. S. White, J. B. Hadley, and J. B. Thompson, Jr., pp. 437–451, Interscience, New York, 1968.

Blackwell, D. D., Heat-flow determinations in the Northwestern United States, *J. Geophys. Res.*, *74*, 992–1007, 1969.

Blackwell, D. D., The thermal structure of the continental crust, in *The Structure and Physical Properties of the Earth's Crust, Geophys. Monogr. Ser.*, vol. 14, edited by J. G. Heacock, pp. 169–184, AGU, Washington, D. C., 1971.

Blackwell, D. D., and C.-G. Baag, Heat flow in a 'blind' geothermal area near Marysville, Montana, *Geophysics*, *38*, 941–956, 1973.

Bunker, C. M., and C. A. Bush, Uranium, thorium, and radium analyses by gamma-ray spectrometry (0.184-0.352 million electron volts), *U.S. Geol. Surv. Prof. Pap. 550-B*, B176–B181, 1966.

Bunker, C. M., and C. A. Bush, A comparison of potassium analyses by gamma-ray spectrometry and other techniques, *U.S. Geol. Surv. Prof. Pap. 575-B*, B164–B169, 1967.

Carslaw, H. S., and J. C. Jaeger, *Conduction of Heat in Solids*, 2nd ed., Oxford University Press, New York, 1959.

Christiansen, R. L., and P. W. Lipman, Cenozoic volcanism and plate-tectonic evolution of the Western United States, 2, Late Cenozoic, *Phil. Trans. Roy. Soc. London, Ser. A, 271*, 249–284, 1972.

Dalrymple, G. B., Potassium-argon dates of three Pleistocene interglacial basalt flows from the Sierra Nevada, California, *Geol. Soc. Amer. Bull., 75*, 753–758, 1964.

Harris, P. G., W. Q. Kennedy, and C. M. Scarfe, Volcanism versus plutonism—The effect of chemical composition, in *Mechanism of Igneous Intrusion, Geol. J. Spec. Issue 2*, edited by G. Newall and N. Rast, pp. 187–200, Gallery Press, Liverpool, England, 1970.

Hildreth, W., and F. Spera, Magma chamber of the Bishop tuff: Gradients in T, P_{total}, and P_{H_2O} (abstract), *Geol. Soc. Amer. Abstr. Programs, 6*, 795, 1974.

Jaeger, J. C., Temperatures outside a cooling intrusive sheet, *Amer. J. Sci., 257*, 44–54, 1959.

Jaeger, J. C., The cooling of irregularly shaped igneous bodies, *Amer. J. Sci., 259*, 721–734, 1961.

Jaeger, J. C., Thermal effects of intrusions, *Rev. Geophys. Space Phys., 2*, 443–466, 1964.

Kistler, R. W., Structure and metamorphism in the Mono Craters quadrangle, Sierra Nevada, California, *U.S. Geol. Surv. Bull., 1221-E*, 53 pp., 1966.

Lachenbruch, A. H., Thermal effects of the ocean on permafrost, *Geol. Soc. Amer. Bull., 68*, 1515–1530, 1957*a*.

Lachenbruch, A. H., Three-dimensional heat conduction in permafrost beneath heated buildings, *U.S. Geol. Surv. Bull., 1052-B*, 51–69, 1957*b*.

Lachenbruch, A. H., Preliminary geothermal model of the Sierra Nevada, *J. Geophys. Res., 73*, 6977–6989, 1968*a*.

Lachenbruch, A. H., Rapid estimation of the topographic disturbance to superficial thermal gradients, *Rev. Geophys. Space Phys., 6*, 365–400, 1968*b*.

Lachenbruch, A. H., Crustal temperature and heat production: Implications of the linear heat-flow relation, *J. Geophys. Res., 75*, 3291–3300, 1970.

Lachenbruch, A. H., M. L. Sorey, R. E. Lewis, and J. H. Sass, The near-surface hydrothermal regime of Long Valley caldera, *J. Geophys. Res., 81*, this issue, 1976.

Lovering, T. S., Theory of heat conduction applied to geological problems, *Geol. Soc. Amer. Bull., 46*, 69–94, 1935.

Nettleton, L. L., Gravity and magnetic calculations, *Geophysics, 7*, 293–310, 1942.

Pakiser, L. C., and R. Robinson, Composition and evolution of the continental crust as suggested by seismic observations, *Tectonophysics, 3*, 547–557, 1966.

Pakiser, L. C., and I. Zietz, Transcontinental crustal and upper-mantle structure, *Rev. Geophys. Space Phys., 3*, 505–520, 1965.

Potter, R. M., Heat flow of the Jemez Plateau (abstract), *Eos Trans. AGU, 54*, 1214, 1973.

Rikitake, T., Studies of the thermal state of the earth, 2, Heat flow associated with magma intrusion, *Bull. Earthquake Res. Inst. Tokyo Univ., 37*, 233–243, 1959.

Roy, R. F., and D. D. Blackwell, Heat flow in the Sierra Nevada and western Great Basin (abstract), *Eos Trans. AGU, 47*, 179–180, 1966.

Roy, R. F., D. D. Blackwell, and F. Birch, Heat generation of plutonic rocks and continental heat flow provinces, *Earth Planet. Sci. Lett., 5*, 1–12, 1968.

Roy, R. F., D. D. Blackwell, and E. R. Decker, Continental heat flow, in *The Nature of the Solid Earth*, edited by E. C. Robertson, pp. 506–543, McGraw-Hill, New York, 1972.

Sass, J. H., A. H. Lachenbruch, R. J. Munroe, G. W. Greene, and T. H. Moses, Jr., Heat flow in the western United States, *J. Geophys. Res., 76*, 6376–6413, 1971*a*.

Sass, J. H., A. H. Lachenbruch, and R. J. Munroe, Thermal conductivity of rocks from measurements on fragments and its application to heat flow determinations, *J. Geophys. Res., 76*, 3391–3401, 1971*b*.

Shaw, H. R., Comments on viscosity, crystal settling, and convection in granitic magmas, *Amer. J. Sci., 263*, 120–152, 1965.

Shaw, H. R., T. L. Wright, D. L. Peck, and R. Okamura, The viscosity of basaltic magma: An analysis of field measurements in Makaopuhi Lava Lake, Hawaii, *Amer. J. Sci., 266*, 225–264, 1968.

Simmons, G., Interpretation of heat flow anomalies, 1, Contrasts in heat production, *Rev. Geophys. Space Phys., 5*, 43–52, 1967*a*.

Simmons, G., Interpretation of heat flow anomalies, 2, Flux due to initial temperature of intrusives, *Rev. Geophys. Space Phys., 5*, 109–120, 1967*b*.

Smith, R. C. T., Conduction of heat in the semi-infinite solid, with a short table of an important integral, *Aust. J. Phys., 6*, 127–130, 1953.

Smith, R. L., and R. A. Bailey, Resurgent cauldrons, Studies in Volcanology, *Geol. Soc. Amer. Mem., 116*, 613–662, 1968.

Sorey, M. L., and R. E. Lewis, Convective heat flow from hot springs in the Long Valley caldera, Mono County, California, *J. Geophys. Res., 81*, this issue, 1976.

Thompson, G. A., The rift system of the western United States, in *The World Rift System, Geol. Surv. of Canada Pap. 66-14*, edited by T. N. Irvine, pp. 280–289, Department of Mines and Technical Surveys, Ottawa, Ontario, 1966.

Thompson, G. A., and D. B. Burke, Regional geophysics of the Basin and Range province, *Ann. Rev. Earth Planet. Sci., 2*, 213–238, 1974.

Uyeda, S., and K. Horai, Terrestrial heat flow in Japan, *J. Geophys. Res., 69*, 2121–2141, 1964.

Van Orstrand, C. E., Flow of heat from an intrusive body into country rock, *Amer. Inst. Mining, Met. Petrol. Eng. Tech. Publ., 1677*, 1–9, 1944.

White, D. E., Geothermal Energy, *U.S. Geol. Surv. Circ., 519*, 17 pp., 1965.

Winkler, H. G. F., and W. Lindemann, The system Qz-Or-An-H_2O within the granitic system Qz-Or-Ab-An-H_2O application to granitic magma formation, *Neues Jahrb. Mineral. Monatsh., 2*, 49–61, 1972.

(Received March 19, 1975;
revised September 15, 1975;
accepted September 15, 1975.)